

WeLa-VAE: Learning Alternative Disentangled Representations Using Weak Labels

Vasilis Margonis Athanasios Davvetas Iraklis A. Klampanos

Institute of Informatics and Telecommunications
National Center for Scientific Research “Demokritos”
Agia Paraskevi 15341, Athens, Greece
{vmargonis, tdavvetas, iaklampanos}@iit.demokritos.gr

Abstract

Learning disentangled representations without supervision or inductive biases, often leads to non-interpretable or undesirable representations. On the other hand, strict supervision requires detailed knowledge of the true generative factors, which is not always possible. In this paper, we consider weak supervision by means of high-level labels that are not assumed to be explicitly related to the ground truth factors. Such labels, while being easier to acquire, can also be used as inductive biases for algorithms to learn more interpretable or alternative disentangled representations. To this end, we propose WeLa-VAE, a variational inference framework where observations and labels share the same latent variables, which involves the maximization of a modified variational lower bound and total correlation regularization. Our method is a generalization of TCVAE, adding only one extra hyperparameter. We experiment on a dataset generated by Cartesian coordinates and we show that, while a TCVAE learns a factorized Cartesian representation, given weak labels of distance and angle, WeLa-VAE is able to learn and disentangle a polar representation. This is achieved without the need of refined labels or having to adjust the number of layers, the optimization parameters, or the total correlation hyperparameter.

1 Introduction

In representation learning, it is often assumed that complex, high-dimensional data, like face photos, are generated by a small number of mutually independent latent variables, usually referred to as generative factors. This assumption implies that such data can be explained by simple explanatory features which are significantly fewer than the original dimensions. Learning representations which identify and separate the few distinct, informative factors of variation is termed as disentanglement. Although a formal definition is currently under debate, a representation is vaguely characterized as disentangled if single features are sensitive to changes in single generative factors, while being relatively invariant to changes in other factors [1]. It has been suggested that disentangled representations, despite their potential on generalizing to diverse downstream tasks, can lead to better understanding of a dataset’s underlying distribution, provide intuition or allow for generative tasks that require “perception”, such as conditional generation [1, 20].

Locatello et al. [22] proved that disentanglement is impossible without inductive biases on both the model and the data, as there exist datasets with multiple sets of generative factors. In the same paper, large-scale experimentation indicated that current unsupervised models cannot reliably learn disentangled representations as the choice of random seeds and hyperparameters seem to have a greater impact than the choice of the model itself. Moreover, the assumption that a disentangled

representation is useful for downstream tasks could not be validated for the considered models and datasets. The authors concluded that future work on disentanglement should deviate from the purely unsupervised setting by making the role of inductive biases and supervision more explicit.

On the other hand, introducing strict supervision requires prior knowledge on the nature or number of the true generative factors. However, this information is often either unavailable or expensive, if not impossible to acquire. For instance, there may exist practical examples of datasets for which no generative factors stand out enough to be recognized upon inspection. In addition, labelling can be laborious and usually targets specific downstream tasks or domain applications, not focusing on the implicit properties of the data. There may be cases where labels reflect generative factors, e.g. digit labels of the MNIST dataset, but this is not generally true in realistic datasets.

An approach that allows the inclusion of supervision while mitigating the difficulties of acquiring ground truth labels is weak supervision. Weak supervision is often provided via weak labels, which may be noisy (e.g. produced by non-experts), partially available (also known as semi-supervision), high-level (dividing the data into fewer classes), or non-corresponding to ground truth. In this paper, we consider the exploitation of weak labels of the last two categories in the context of disentanglement. This information can act as inductive bias for learning disentangled representations, without posing the restrictions of strict supervision or the pitfalls of unsupervised practices. Moreover, weak supervision may lead to representations that are impossible for unsupervised models to learn, hence more interpretable and potentially useful for downstream tasks.

In this paper we contribute:

1. WeLa-VAE, a scalable framework based on Variational Auto-encoders [17] with *total correlation* regularization, that leverages weak labels towards learning disentangled representations.
2. A synthetic dataset of images depicting white Gaussian blobs on a black canvas, along with appropriate weak labels to support our experiments.
3. A thorough quantitative and qualitative evaluation, and comparison of the models used for the considered tasks based on a suitable novel and generalizable metric.

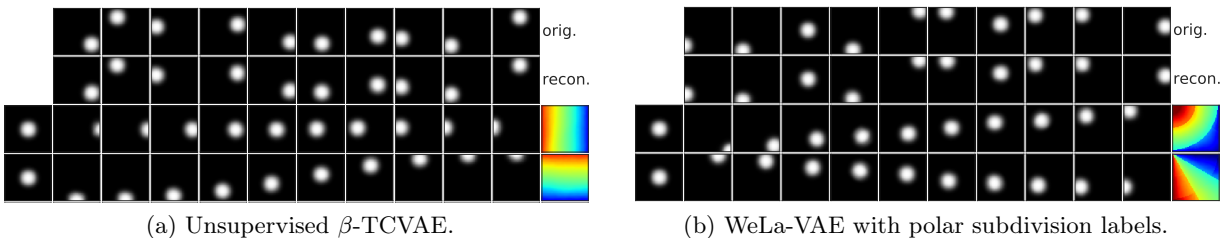


Figure 1: β -TCVAE and WeLa-VAE trained on Blobs dataset. First row: original images. Second row: corresponding reconstructions. Rest: latent traversals in $[-3, +3]$. Left-most column: Image before traversal. Heat maps show the mean activation of each channel, as a function of position (dark blue, green, and dark red correspond to -3 , 0 and $+3$, respectively).

Next section discusses related work. In section 3 we describe the derivation and implementation of WeLa-VAE. In Section 4, we introduce the dataset, provide details about the evaluation method and discuss the performance of WeLa-VAE next to a baseline established by β -TCVAE. Finally, we highlight the strengths and weaknesses of our framework, and propose directions for future work in section 5.

2 Related Work

The literature on learning disentangled representations can be divided in unsupervised and supervised learning frameworks. Unsupervised models are trained without available information about the number or the nature of the generative factors. Notable earlier approaches based on spike-and-slab restricted Boltzmann machines [8], tensor analyzers [26] and commutative Lie groups [6], produced promising results, albeit failing to scale well on big datasets. InfoGAN [5] although scalable, inherits training instability and mode jumping from GAN [11].

Kingma and Welling [17] introduced variational auto-encoders (VAEs) as a scalable framework for variational Bayesian inference. In VAE, a two-step generative process is assumed where a latent vector z is sampled from an isotropic Gaussian prior $p(z) = \mathcal{N}(0, \mathbf{I})$ and observations x are sampled from the posterior $p_\theta(x|z)$. The distribution $p_\theta(z|x)$ is approximated by a variational distribution $q_\phi(z|x)$. Both $p_\theta(x|z)$ and $q_\phi(z|x)$ are parameterized by neural-networks, which are jointly trained by maximizing the variational lower bound (ELBO) of $\log p_\theta(x)$ for all observations x :

$$\text{ELBO}(\theta, \phi) = -\text{KL}(q_\phi(z|x) || p(z)) + \mathbb{E}_{z \sim q_\phi}[\log p_\theta(x|z)]. \quad (1)$$

State-of-the-art unsupervised methods for disentanglement are variants of VAE which enforce a factorized aggregated posterior $q_\phi(z) = \int q_\phi(z|x)p_\theta(x)dx$. In β -VAE [12] a Lagrange multiplier on the KL term introduces an information bottleneck on the latent channel with a trade-off in reconstruction quality. Burgess et al. [3] proposed to incrementally increase the latent channel capacity for better reconstructions. Independently, FactorVAE [14] and β -TCVAE [4] augment the VAE objective (1) with a regularizer that penalizes the *total correlation* $\text{KL}(q(z) || \prod_k q(z_k))$. DIP-VAE [19] uses a similar augmentation which enforces the moments of $q(z)$ and the isotropic Gaussian prior $p(z)$ to match.

Locatello et al. [22] performed a large-scale empirical study on the unsupervised setting involving VAE variants [12, 3, 14, 4, 19], disentanglement metrics [12, 14, 9, 19, 4, 24] and synthetic datasets. Their experimental results indicate that the choice of hyperparameters and random seeds is more significant than model selection on the learned representations and metric scores, and that good random seeds and hyperparameters cannot be identified without access to ground-truth labels. They suggest that unsupervised learning of disentangled representation is unreliable and motivate future work that focuses on inductive biases and explicit supervision. WeLa-VAE framework is a step towards that direction.

In the supervised scheme, factors of interest are explicitly labelled, and information about their nature (e.g. categorical or continuous) is available. However, obtaining explicit labels is problematic, therefore most models are either semi or weakly supervised. For example, Kingma et al. [16], Narayanaswamy et al. [23] and Yan et al. [28] propose semi-supervised variants of VAEs where observed labels are treated as latent variables. Other approaches considered various forms of weak supervision, i.e., implicit information about the factors of variation, including temporal coherence [7, 13, 27], rendering knowledge in computer graphics [18], and leveraging groups of observations where the generative factors are constant [2, 10, 25]. In contrast to existing supervised approaches, we provide weak supervision by high-level labels which are neither assumed to be explicitly related to the ground truth factors, nor are they treated as latent variables.

3 WeLa-VAE Framework

Let $\mathcal{D} = \{X, \mathcal{Y} = (Y_1, \dots, Y_m)\}$ be a dataset consisting of observations $x \in \mathbb{R}^D$ and m weak labels y_1, \dots, y_m per observation. That is, for every x^i we have a corresponding multi-label $y^i = (y_1^i, \dots, y_m^i)$.

Given such a dataset, our objective is to obtain a disentangled representation of x that is influenced by y . Given that the labels are related to the observations, it is reasonable to consider the case where y shares the same latent variables with x . Therefore, we assume an extended generative model depicted in Figure 2, which is similar to that of VAE [17], with the addition of one variable for each label. More specifically, a latent variable is first sampled from a distribution $p(z)$. Then, x and $y = (y_1, \dots, y_m)$ are sampled from the conditionals $p_\theta(x|z)$ and $p_\theta(y|z) = \prod_j p_\theta(y_j|z)$, respectively.

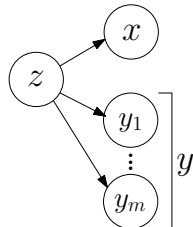


Figure 2: Generative model

A suitable objective function could be the maximization of the log-likelihood of $p_\theta(x, y)$. Using an auxiliary distribution $q_\phi(z|x, y)$ to approximate the intractable posterior $p_\theta(z|x, y)$, allows us to obtain a tractable variational lower bound¹ on the log-probability:

$$\begin{aligned} \log p_\theta(x, y) &\geq \mathbb{E}_{z \sim q_\phi}[\log p_\theta(x|z)] + \mathbb{E}_{z \sim q_\phi}[\log p_\theta(y|z)] - \text{KL}(q_\phi(z|x, y) \parallel p(z)) \\ &= \mathbb{E}_{z \sim q_\phi}[\log p_\theta(x|z)] + \sum_{j=1}^m \mathbb{E}_{z \sim q_\phi}[\log p_\theta(y_j|z)] - \text{KL}(q_\phi(z|x, y) \parallel p(z)). \end{aligned} \quad (2)$$

However, we are not interested in the exact value of the log-probability, as our objective is to obtain disentangled representations that are influenced by the weak-labels. Therefore, we choose to optimize a modified variational lower bound. More specifically, to ensure that the labels are reconstructed properly, we add a multiplier hyperparameter $\gamma \geq 1$ on the labels' reconstruction term to control its relative scale to the rest of the terms:

$$\gamma \text{ELBO}(\theta, \phi) := \mathbb{E}_{z \sim q_\phi}[\log p_\theta(x|z)] + \gamma \cdot \sum_{j=1}^m \mathbb{E}_{z \sim q_\phi}[\log p_\theta(y_j|z)] - \text{KL}(q_\phi(z|x, y) \parallel p(z)). \quad (3)$$

Moreover, as in [14, 4], to enforce a factorized aggregated posterior

$$q_\phi(z) = \iint q_\phi(z|x, y) \cdot p_\theta(x) \cdot p_\theta(y) \, dx dy,$$

we introduce a total correlation regularizer controlled by a hyperparameter $\beta \geq 0$. Since this term is intractable, we use the biased Monte-Carlo estimator proposed in β -TCVAE [4]. Note that WeLa-VAE generalizes easily to different ways of forcing a factorized aggregated posterior. For example, one may substitute the total correlation penalty with the regularizers of DIP-VAE [19]. The objective function of WeLa-VAE is

$$\min \mathcal{L}(\theta, \phi) = -\mathbb{E}_{x, y}[\gamma \text{ELBO}(\theta, \phi)] + \beta \cdot \text{KL}(q_\phi(z) \parallel \prod_{k=1}^K q_\phi(z_k)). \quad (4)$$

We postulate that this method results in representations which are strongly affected by the labels, as the network is forced to gain the discriminative ability to reconstruct the labels accurately.

¹See Appendix A

Meanwhile, the total correlation penalty encourages the representation to factorize. As in most variants of VAE’s, the distributions $q_\phi(z|x, y)$, $p_\theta(x|z)$ and $p_\theta(y|z)$ are parameterized by two neural networks, one for $q_\phi(z|x, y)$ (encoder) and one for both $p_\theta(x|z)$ and $p_\theta(y|z)$ (decoder). The prior $p(z)$ is set to the non-parametric isotropic Gaussian $\mathcal{N}(0, \mathbf{I})$ and $q_\phi(z|x, y)$ is also a diagonal Gaussian $\mathcal{N}(\mu, \sigma^2 \mathbf{I})$. Sampling from $q_\phi(z|x, y)$ is done via the reparameterization trick, i.e. $z = \mu + \sigma \odot \epsilon$, where $\epsilon \sim \mathcal{N}(0, \mathbf{I})$. The choice of family of distributions for $p_\theta(x|z)$ and $p_\theta(y|z)$ depends on the nature of the dataset. During our implementation of WeLa-VAE, x and y are concatenated as a single input in a stacked dense autoencoder. However, the implementation of WeLa-VAE can be versatile, allowing for the utilisation of the intrinsic properties of any given dataset. For instance, WeLa-VAE can be adapted to implementations that utilise the spatial aspect of a dataset, such as convolutional layers, by concatenating weak labels along with the first dense layer representations of x .

4 Experiments

In this section, we introduce a dataset for experimentation, provide details about the experimental parameters and evaluation method and discuss the performance of WeLa-VAE compared to a baseline established by β -TCVAE.

4.1 Evaluation Dataset

We test WeLa-VAE on a synthetic dataset of 64×64 images containing a white Gaussian blob positioned on a black canvas (Figure 3a). A similar dataset has appeared in the context of disentanglement in [3]. In our case, the use of weak labels and the evaluation methodology necessitated the creation of a new dataset. The generative factors are the Cartesian coordinates of the blob’s center on the canvas. For every possible position, we sample 25 different Gaussian blobs, getting a total of $N = 102,400$ images, which is the training set X . This is a motivating example because the observed images can be also explained in polar coordinates, therefore its a case of a dataset which has two different, but equally valid sets of generative factors. Our objective is to provide WeLa-VAE with weak labels indicating angle and distance, expecting to obtain a disentangled polar representation. Assuming that $(0, 0)$ lies at the top left corner of the canvas, we construct two membership labels, one for angle and one for distance, for every image (Figure 3b). To this end, the canvas is divided in p disjoint areas, and the label vector is the one-hot encoding of the label associated with the area that the center of the blob lies in. The value p determines the dimension of the one-hot encoded label vectors, and it is very important in this context as it empirically indicates the amount of bias introduced by the labels: Higher p means that more decision boundaries must be learned by the network to reconstruct the labels accurately. Hence, to test the effect of label dimensionality on the learned representations, we construct labels for $p = 2, 3, \dots, 8$.

4.2 Evaluation

We consider two tasks: (1) learning a factorized Cartesian representation and (2) learning a factorized polar representation. We use latent traversals and positional heat maps as a means of qualitative evaluation. Quantitative evaluation of WeLa-VAE is not trivial and known disentanglement metrics are not suitable in this case. Specifically, such metrics measure various notions of statistical relation between the learned representation and the ground truth factors, which is unfit for the second task of learning a polar representation. Thus, we choose to measure performance as the ability of approximating the true Cartesian coordinates (c_1, c_2) used to generate an image x , by a simple

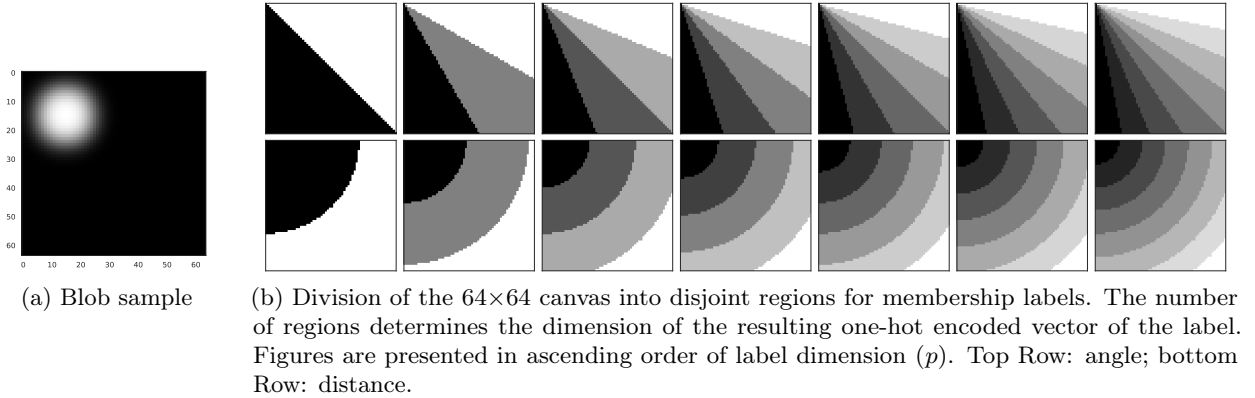


Figure 3: Blobs dataset sample and division of canvas for weak labels.

transformation of the learned latent space. Note that we use the mean vector μ of the Gaussian encoder as the representation, not the sample z .

For the task of learning a factorized Cartesian representation, an ideal model learns a representation μ with one channel μ_i corresponding to c_1 and one μ_j corresponding to c_2 . An approximation $(\tilde{c}_1, \tilde{c}_2)$ can be computed by simply mapping the feature value ranges to $[0, 64]$ linearly:

$$\begin{aligned}\tilde{c}_1 &= (\mu_i - \min(\mu_i)) \cdot (64 / (\max(\mu_i) - \min(\mu_i))), \\ \tilde{c}_2 &= (\mu_j - \min(\mu_j)) \cdot (64 / (\max(\mu_j) - \min(\mu_j))).\end{aligned}\tag{5}$$

For the second task, we approximate (c_1, c_2) as in a similar fashion: Let μ_i correspond to angle ϕ and μ_j correspond to distance d . First, we compute

$$\begin{aligned}\mu_\phi &= (\mu_i - \min(\mu_i)) \cdot ((\pi/2) / (\max(\mu_i) - \min(\mu_i))), \\ \mu_d &= (\mu_j - \min(\mu_j)) \cdot (90.5 / (\max(\mu_j) - \min(\mu_j))),\end{aligned}\tag{6}$$

to ensure that the values lie in a valid range. Since $c_1, c_2 \in [0, 64]$, then $d \in [0, 90.5]$ and $\phi \in [0, \pi/2]$. Then, we apply the known mapping from polar to Cartesian coordinates,

$$\begin{aligned}\tilde{c}_1 &= \mu_d \cdot \cos(\mu_\phi), \\ \tilde{c}_2 &= \mu_d \cdot \sin(\mu_\phi).\end{aligned}\tag{7}$$

We measure approximation as the mean squared $L2$ error of (c_1, c_2) from $(\tilde{c}_1, \tilde{c}_2)$, across all samples. However, there is no way of knowing which channels to assign to angle and distance without qualitative inspection. Moreover, it is possible for the encoder to invert the order of values, e.g. blobs in distance close to 0 represented by high positive values instead of low negative, and vice versa. Therefore, we try all possible assignments and inversions and return the lowest MSE. For the task of learning a Cartesian representation, we take approximations via equations (5) and measure MSE, while for the task of learning a polar representation, we use equations (6) and (7). This evaluation protocol easily generalizes to other tasks where certain representation qualities are expected.

4.3 Experimental setup

Images are valued in $[0, 1]$, therefore we parameterize the distribution $p_\theta(x|z)$ as a multivariate Bernoulli. One-hot encoded labels are binary vectors thus $p_\theta(y|z)$ is parameterized as categorical.

In all experiments, both encoder and decoder consist of two fully-connected, 1200–neuron layers. Training is done using the Adam optimizer [15] with learning rate 10^{-4} , in batches of size 256 for 150 epochs². We set $\beta=40$ for both TCVAE and WeLa-VAE to showcase that good β values can be transferred. As we measure reconstruction error with cross-entropy for both images and labels, we choose γ such that

$$\text{Image Dimension} \approx \gamma \times \text{Label Dimension},$$

to ensure that image and label reconstructions are of similar scale. Although this rule-of-thumb proved sufficient for the concerned dataset and task, searching for γ can also be done through label reconstruction loss, e.g., choosing a value γ that results in accuracy greater than some specified threshold. Eight models are tested; one TCVAE with latent channel size $K=5$, and one WeLa-VAE with $K=2$ for every label dimensionality p^3 . We train each model for 50 different types of random weight initialization and report the scores for each task. We also visualize the representations that achieve the lowest MSEs.

4.4 Results

We find that β -TCVAE for $\beta = 40$ is able to learn a disentangled Cartesian representation without using unnecessary channels. As expected, the model is heavily dependent on random seeds [22], as some learned representations were entangled and non-interpretable. Our specified MSE score used for the task of learning a Cartesian representation, was able to identify “good” and “bad” models. In Figure 4, we visualize the latent traversals and positional heat maps of the models that achieved the lowest (Figure 4a) and highest (Figure 4b) MSE out of 50 random weight initializations. Evidently, the best model has clearly learnt the desired representation, in contrast to the worst model, where the representations are entangled and one redundant channel has been opened.

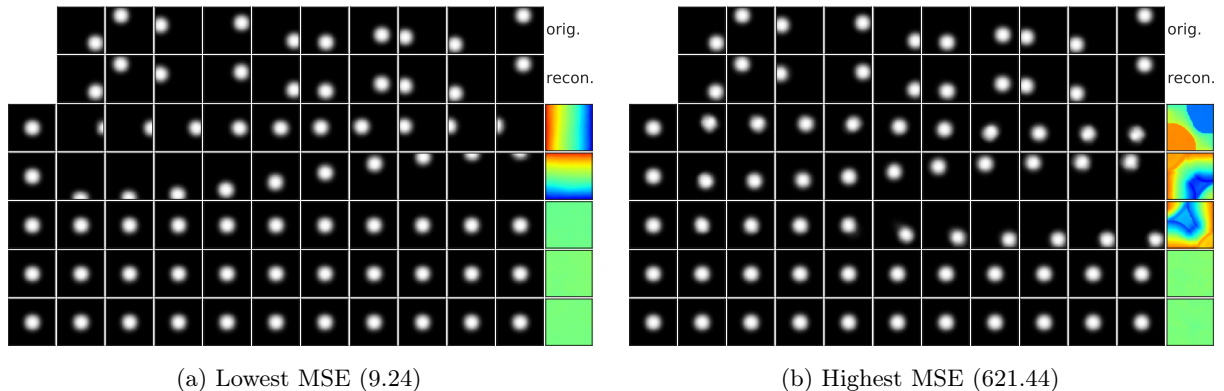


Figure 4: Visualization of representations learned by β -TCVAE with lowest and highest MSE out of 50 random seeds, measured for the task of learning the true Cartesian generative factors.

For the task of learning a polar representation, we reused the same network and training configuration, as well as the β value from the model of Figure 4a and trained WeLa-VAE for various label dimensionalities. Table 1 sums up the scores of all models considered for this task, including the training accuracy of angle and distance of the best models. The latent traversals and heat maps

²Each epoch takes approximately 9 seconds on a GeForce 1080Ti.

³Choosing $K > m$ produced sub-optimal results, as redundant channels were opened, leading to entangled representations. Allowing for arbitrarily large K is left as future work.

of the best models for TCVAE and WeLa-VAE are also shown in Figure 5. WeLa-VAE was able to recover a clear polar representation for some label dimensionalities, suggesting that architectures and hyperparameters from unsupervised models can be transferred to WeLa-VAE, with the only requirement being the tuning of γ . Moreover, label reconstruction error is low for all WeLa-VAE models, with training accuracy close to 100% for both angle and distance, without compromising image reconstructions, which is of a similar quality to TCVAE. As above, our evaluation metric identifies models whose representations exhibit the desired properties, i.e. representations with the best scores are the ones closer to being polar. Indicatively, the model that learned the best representation uses a label dimensionality of $p = 3$ (Figure 5c), and is also the one achieving the total lowest MSE. On the other hand, no unsupervised TCVAE succeeded in effectively learning a polar representation.

However, MSEs indicate that WeLa-VAE is also heavily dependent on random seeds. Evidently, “good” models are scarce, with mean MSE being significantly greater than lowest MSE for all models. Moreover, there is no evidence that higher label dimensionality p had a positive effect on the representations, at least for the considered dataset. On the contrary, better scores were obtained for low p values, namely $p = 2$ and $p = 3$. Although $p = 3$ yielded the best overall result, mean MSE and mean MSE of top 5 scores are significantly lower for $p = 2$, compared to all p values, meaning less sensitivity to random seeds and more frequent learning of “good” representations.

Table 1: MSE scores on the task of learning a polar representation. For each model, we provide the hyperparameters and label dimensionality (p) used for training. We report the lowest, overall mean and mean of the best 10% of scores, across 50 random seeds. We also report the training accuracy on angle (ϕ) and distance (d) labels of the model with the lowest MSE.

Model	Parameters			Accuracy		MSE		
	β	γ	Label dim.	ϕ	d	Lowest	Mean	Mean: best 10%
β -TCVAE	40	-	-	-	-	239.76	435.68	286.14
WeLa-VAE	40	2000	$p=2$	0.99	1.00	83.47	255.28	94.30
		1500	$p=3$	0.99	1.00	40.28	824.88	295.24
		1000	$p=4$	0.99	1.00	95.80	751.90	348.86
		800	$p=5$	0.99	1.00	176.04	797.66	449.22
		750	$p=6$	0.99	1.00	179.52	711.45	315.62
		600	$p=7$	0.99	1.00	190.44	686.62	352.51
		500	$p=8$	0.99	1.00	160.74	659.80	275.18

5 Conclusion and future work

We propose WeLa-VAE, a framework where weak labels are used to provide inductive biases towards disentanglement. Our method is derived by assuming an extended generative model where labels y and observations x share the same latent variables. The objective function is a modified variational lower bound of $\log p_{\theta}(x, y)$ with a weighted label reconstruction loss, coupled with a total correlation regularizer [14, 4] to enforce a factorized aggregated posterior. We experiment with WeLa-VAE on a synthetic dataset consisting of images with two generative factors; Cartesian coordinates, for which a β -TCVAE model learns a disentangled, axis-aligned Cartesian representation. Reusing the same

architecture, optimization parameters and β value of TCVAE, we provide WeLa-VAE with one-hot labels of varying dimension that indicate angle and distance. We measure the performance of WeLa-VAE as the mean squared L2 error of the true generative factor values from an approximation obtained by a simple transformation of the learned representations. This evaluation protocol discriminates representations with the desired qualities. We find that WeLa-VAE successfully learns a disentangled polar representation with the cost of tuning only one extra hyperparameter. Moreover, the best models used labels of low dimension, suggesting that WeLa-VAE does not need refined labels to perform well. This shows that, weak supervision in the form of high-level labels provides the necessary inductive biases towards learning alternative and more interpretable disentangled representations.

An immediate application of WeLa-VAE is to aid interpretability, allowing for systematic and provable elicitation of alternative sets of interpretable and disentangled-enough representations. An additional application of WeLa-VAE is related to the assumption that disentangled representations can lead to better performance on downstream tasks. We expect that disentangled representations learned by WeLa-VAE can be useful for downstream tasks which relate to the given weak labels. One limitation of WeLa-VAE is the requirement that latent channel size K must be equal to the number of labels m , which is left as future work. Moreover, the assumption of fully-observing the labels may be unrealistic in some scenarios. We conjecture that a variation of WeLa-VAE where labels are partially-observed would produce comparable results, which is currently under investigation. Finally, an interesting direction for future work would be to remove the labels from the input layer of the encoder and let the decoder do all the work. Such a network could be trained in a dynamic setting where the labels become available incrementally and for a short amount of time, using learning-without-forgetting techniques [21].

References

- [1] Y. Bengio, A. Courville, and P. Vincent. Representation learning: A review and new perspectives. *IEEE Transactions on Pattern Analysis and Machine Intelligence*, 35(8):1798–1828, 2013.
- [2] Diane Bouchacourt, Ryota Tomioka, and Sebastian Nowozin. Multi-level variational autoencoder: Learning disentangled representations from grouped observations. In *AAAI Conference on Artificial Intelligence*, 2018.
- [3] Christopher P. Burgess, Irina Higgins, Arka Pal, Loïc Matthey, Nick Watters, Guillaume Desjardins, and Alexander Lerchner. Understanding disentangling in β -vae. *ArXiv preprint*, ArXiv:1804.03599, 2018.
- [4] Tian Qi Chen, Xuechen Li, Roger B. Grosse, and David Duvenaud. Isolating sources of disentanglement in variational autoencoders. In *Advances in Neural Information Processing Systems*, 2018.
- [5] Xi Chen, Yan Duan, Rein Houthoofd, John Schulman, Ilya Sutskever, and Pieter Abbeel. Infogan: Interpretable representation learning by information maximizing generative adversarial nets. In *Advances in Neural Information Processing Systems*, 2016.
- [6] Taco Cohen and Max Welling. Learning the irreducible representations of commutative lie groups. In *International Conference on Machine Learning*, 2014.
- [7] Emily L. Denton and Vighnesh Birodkar. Unsupervised learning of disentangled representations from video. In *Advances in Neural Information Processing Systems*, 2017.
- [8] Guillaume Desjardins, Aaron C. Courville, and Yoshua Bengio. Disentangling factors of variation via generative entangling. *ArXiv preprint*, ArXiv:1210.5474, 2012.
- [9] Cian Eastwood and Christopher K. I. Williams. A framework for the quantitative evaluation of disentangled representations. In *International Conference on Learning Representations*, 2018.
- [10] Zunlei Feng, Xinchao Wang, Chenglong Ke, Anxiang Zeng, Dacheng Tao, and Mingli Song. Dual swap disentangling. In *Advances in Neural Information Processing Systems*, 2018.

- [11] Ian J. Goodfellow, Jean Pouget-Abadie, Mehdi Mirza, Bing Xu, David Warde-Farley, Sherjil Ozair, Aaron C. Courville, and Yoshua Bengio. Generative adversarial nets. In *Advances in Neural Information Processing Systems*, 2014.
- [12] Irina Higgins, Loïc Matthey, Arka Pal, Christopher Burgess, Xavier Glorot, Matthew Botvinick, Shakir Mohamed, and Alexander Lerchner. beta-vae: Learning basic visual concepts with a constrained variational framework. In *International Conference on Learning Representations*, 2017.
- [13] Wei-Ning Hsu, Yu Zhang, and James R. Glass. Unsupervised learning of disentangled and interpretable representations from sequential data. In *Advances in Neural Information Processing Systems*, 2017.
- [14] Hyunjik Kim and Andriy Mnih. Disentangling by factorising. In *International Conference on Machine Learning*, 2018.
- [15] Diederik P. Kingma and Jimmy Ba. Adam: A method for stochastic optimization. In *International Conference on Learning Representations*, 2015.
- [16] Diederik P. Kingma, Shakir Mohamed, Danilo Jimenez Rezende, and Max Welling. Semi-supervised learning with deep generative models. In *Advances in Neural Information Processing Systems*, 2014.
- [17] Diederik P. Kingma and Max Welling. Auto-encoding variational bayes. In *International Conference on Learning Representations*, 2014.
- [18] Tejas D. Kulkarni, William F. Whitney, Pushmeet Kohli, and Joshua B. Tenenbaum. Deep convolutional inverse graphics network. In *Advances in Neural Information Processing Systems*, 2015.
- [19] Abhishek Kumar, Prasanna Sattigeri, and Avinash Balakrishnan. Variational inference of disentangled latent concepts from unlabeled observations. In *International Conference on Learning Representations*, 2018.
- [20] Brenden M. Lake, Tomer D. Ullman, Joshua B. Tenenbaum, and Samuel J. Gershman. Building machines that learn and think like people. *Behavioral and Brain Sciences*, 40:e253, 2017.
- [21] Zhizhong Li and Derek Hoiem. Learning without forgetting. *IEEE Trans. Pattern Anal. Mach. Intell.*, 40(12):2935–2947, 2018.
- [22] Francesco Locatello, Stefan Bauer, Mario Lucic, Gunnar Rätsch, Sylvain Gelly, Bernhard Schölkopf, and Olivier Bachem. Challenging common assumptions in the unsupervised learning of disentangled representations. In *International Conference on Machine Learning*, 2019.
- [23] Siddharth Narayanaswamy, Brooks Paige, Jan-Willem van de Meent, Alban Desmaison, Noah D. Goodman, Pushmeet Kohli, Frank D. Wood, and Philip H. S. Torr. Learning disentangled representations with semi-supervised deep generative models. In *Advances in Neural Information Processing Systems*, 2017.
- [24] Karl Ridgeway and Michael C. Mozer. Learning deep disentangled embeddings with the f-statistic loss. In *Advances in Neural Information Processing Systems*, 2018.
- [25] Adria Ruiz, Oriol Martínez, Xavier Binefa, and Jakob Verbeek. Learning disentangled representations with reference-based variational autoencoders. *ArXiv preprint*, ArXiv:1901.08534, 2019.
- [26] Yichuan Tang, Ruslan Salakhutdinov, and Geoffrey E. Hinton. Tensor analyzers. In *International Conference on Machine Learning*, 2013.
- [27] Ruben Villegas, Jimei Yang, Seunghoon Hong, Xunyu Lin, and Honglak Lee. Decomposing motion and content for natural video sequence prediction. In *International Conference on Learning Representations*, 2017.
- [28] Xinchen Yan, Jimei Yang, Kihyuk Sohn, and Honglak Lee. Attribute2image: Conditional image generation from visual attributes. In *European Conference on Computer Vision (ECCV)*, 2016.

A Variational Lower Bound

The generative model related to WeLa-VAE consists of $m + 2$ random variables, z , x and $y = (y_1, \dots, y_m)$. First, the latent variable z is sampled from a prior distribution $p(z)$. Then, both x and y , which are conditionally independent with respect to z , are sampled from the posteriors $p_\theta(x|z)$ and $p_\theta(y|z) = \prod_{j=1}^m p_\theta(y_j|z)$, respectively. We are interested in obtaining a variational lower bound on the log-likelihood of the joint distribution $p_\theta(x, y)$.

Applying the chain rule yields

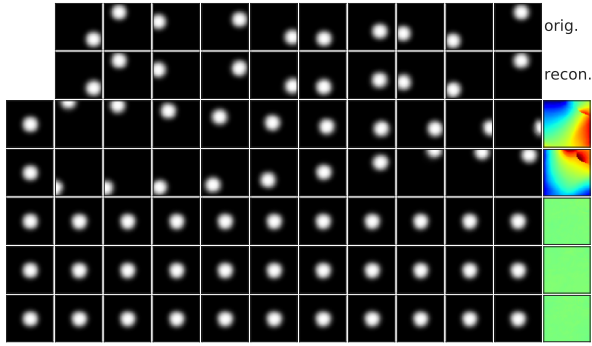
$$\log p_\theta(x, y) = \log \frac{p_\theta(y, x, z)}{p_\theta(z|x, y)} = \log \frac{p_\theta(y|z) \cdot p_\theta(x|z) \cdot p(z)}{p_\theta(z|x, y)}.$$

Then, we introduce the auxiliary distribution $q_\phi(z|x, y)$ which approximates the intractable $p_\theta(z|x, y)$ on the right-hand side, and take the expectation over all z sampled from $q_\phi(z|x, y)$, which gives

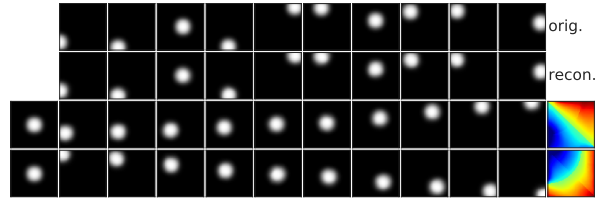
$$\begin{aligned} \mathbb{E}_{z \sim q_\phi}[\log p_\theta(x, y)] &= \mathbb{E}_{z \sim q_\phi} \left[\log \frac{p_\theta(y|z) \cdot p_\theta(x|z) \cdot p(z)}{p_\theta(z|x, y)} \cdot \frac{q_\phi(z|x, y)}{q_\phi(z|x, y)} \right] \\ &= \mathbb{E}_{z \sim q_\phi} \left[\log \frac{q_\phi(z|x, y)}{p_\theta(z|x, y)} \right] + \mathbb{E}_{z \sim q_\phi} \left[\log \frac{p_\theta(y|z) \cdot p_\theta(x|z) \cdot p(z)}{q_\phi(z|x, y)} \right] \\ &= \text{KL}(q_\phi(z|x, y) \parallel p_\theta(z|x, y)) + \mathbb{E}_{z \sim q_\phi} \left[\log \frac{p_\theta(y|z) \cdot p_\theta(x|z) \cdot p(z)}{q_\phi(z|x, y)} \right]. \end{aligned}$$

Since KL divergence is non-negative and $p_\theta(x, y)$ is constant with respect to z ,

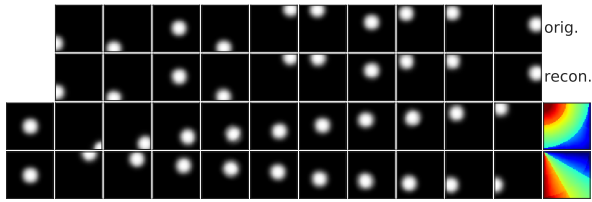
$$\begin{aligned} \log p_\theta(x, y) &\geq \mathbb{E}_{z \sim q_\phi} \left[\log \frac{p_\theta(y|z) \cdot p_\theta(x|z) \cdot p(z)}{q_\phi(z|x, y)} \right] \\ &= \mathbb{E}_{z \sim q_\phi}[\log p_\theta(x|z)] + \mathbb{E}_{z \sim q_\phi}[\log p_\theta(y|z)] + \mathbb{E}_{z \sim q_\phi} \left[-\log \frac{q_\phi(z|x, y)}{p(z)} \right] \\ &= \mathbb{E}_{z \sim q_\phi}[\log p_\theta(x|z)] + \mathbb{E}_{z \sim q_\phi}[\log p_\theta(y|z)] - \text{KL}(q_\phi(z|x, y) \parallel p(z)). \end{aligned}$$



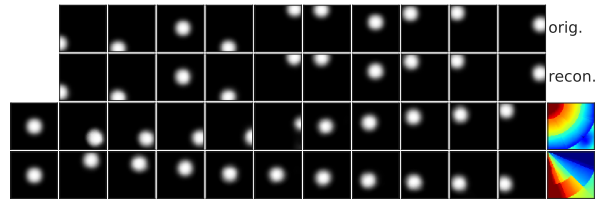
(a) TCVAE: no labels, MSE=239.76



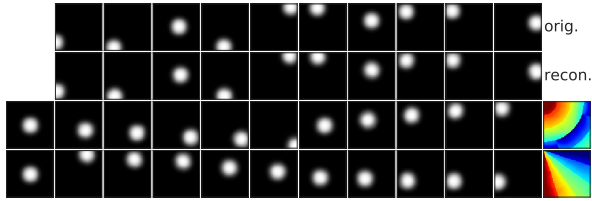
(b) WeLa-VAE: $p=2$, $\gamma=2000$, MSE=83.47



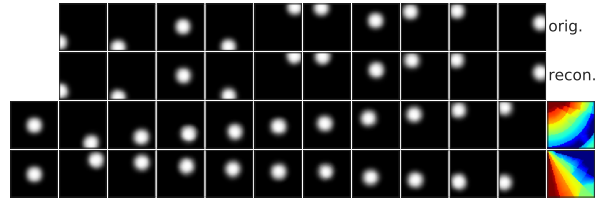
(c) WeLa-VAE: $p=3$, $\gamma=1500$, MSE=40.28



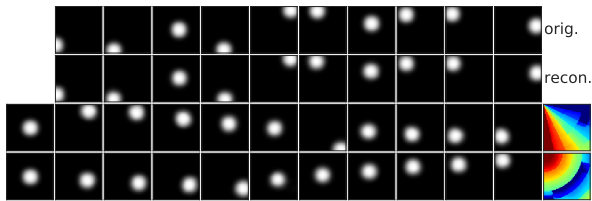
(d) WeLa-VAE: $p=4$, $\gamma=1000$, MSE=95.80



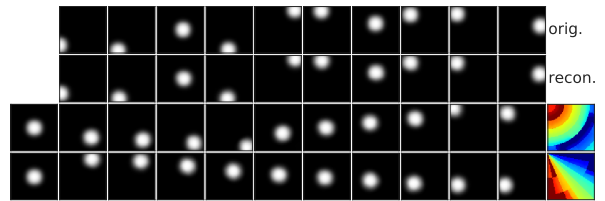
(e) WeLa-VAE: $p=5$, $\gamma=800$, MSE=176.04



(f) WeLa-VAE: $p=6$, $\gamma=750$, MSE=179.52



(g) WeLa-VAE: $p=7$, $\gamma=600$, MSE=190.44



(h) WeLa-VAE: $p=8$, $\gamma=500$, MSE=160.74

Figure 5: WeLa-VAE trained on Blobs dataset with angle and distance labels of different dimensionality p . Each sub-figure visualizes the representations of the model with the lowest MSE out of 50 random seeds.